Estimating winter albedo in dairy agroecosystems for researchers conducting plot-scale studies: A technical report

INTRODUCTION AND OBJECTIVE

Nutrient losses from agricultural runoff is one of the leading causes of surface water impairment from a nonpoint source, thus is a continued priority for agricultural research and policy (Carpenter et al., 1998; USEPA, 2015; Parris, 2011). In the temperate United States and Canada, approximately half of annual runoff volumes are generated during the winter (Stuntebeck et al., 2011), with runoff up to four times greater on frozen versus unfrozen soils (Good et al., 2012). Therefore, nutrient management is important beyond the growing season and particularly to wintertime land-applications of manure, a longstanding practice for many dairy producers (Srinivasan et al., 2006). Investigating the year-round management of dairy agroecosystems, however, necessitates a mechanistic field evaluation of runoff generation and nutrient loading on land with winter-applied manure.

Process-level approaches have been impeded by a lack of field methodology that functions both at the plot-sale and under frozen conditions. In this study, a method was needed to repeatedly estimate albedo across 18 plots throughout two winters. Albedo is an important measurement for winter research because it represents the surface reflection of solar radiation, which drives most snowmelt and is likely to change with applications of manure. To measure albedo, one of two methods is generally used: satellite data (e.g. MODIS, LANDSAT) or field instrumentation with a net radiometer. Satellite methods are inappropriate for most plot-scale studies because the finest resolution of the data is 30 m. Net radiometers provide robust field measurements of albedo, but are often too costly (i.e. > $4000 per unit) and at most, one is generally installed per field. This study investigated multiple manure and land management practices across 18 plots, thus albedo needed to be repeatedly measured across each plot throughout winter seasons. Installing 18 net radiometers was cost-prohibitive and the frequent movement of net radiometers between plots is problematic because of their fragility and the extreme conditions of the winter environment (i.e. subzero temperatures, high winds, and icy terrain). However, most of the solar energy reflected by snowpack is within the visible band of the electromagnetic spectrum, making digital imagery a strong and inexpensive option for plot-scale albedo estimates (Corripio, 2004). Therefore, the objective of this product is to demonstrate a cost-effective and practical field approach to measure albedo in plot-scale, agricultural settings during winter. Specifically, we developed a multiple linear regression (MLR) model of digital imagery, surface and weather conditions, and known albedo values.

MATERIALS AND METHODS

Site Description and Field Experiments

The field study was conducted at the University of Wisconsin – Madison Arlington Agricultural Research Station (43˚17’ N 89˚21’ W) as part of a larger investigation of surface nutrient transport in actively-managed dairy agroecosystems during the non-growing season. 18 plots (5 x 15 m each) were established on a south-facing, 5.8 % sloped field that was cropped with continuous corn for silage. Approximately 20 rows of corn were planted along the contour in each plot. The field is predominantly a Saybrook silt loam (fine-silty, mixed, superactive, mesic Oxyaquic Argiudoll), with a Ringwood silt loam (fine-loamy, mixed, superactive, mesic Typic Argiudoll), and a Griswald silt loam (fine-loamy, mixed, superactive, mesic Typic Argiudoll). Soil organic matter content is 4.0 % (SE = 0.04) at a 0 – 2.5 cm depth.

The plots followed a complete factorial arrangement (2 tillage treatments x 3 manure timing treatments) in triplicate for two winter seasons (2015-2016 and 2016-2017) to test the snowmelt dynamics and

hydrology of frozen soils from common management practices (Figure 1). The tillage treatments included a conventional tillage with fall chisel plow and a spring finisher (CT) and no-tillage (NT), which resulted in rough versus smooth soil surfaces, respectively. The typical timing of winter manure applications were represented with three manure treatments: 1) an early-December application at the typical onset of the freezing season D), 2) a late-January application midway through the freezing season (J), and 3) an unmanured control (C). The full treatments are abbreviated as conventional tillage with no manure (control): CTC, conventional tillage with a December manure application: CTD, conventional tillage with a January manure application: CTJ, no-tillage with no manure (control): NTC, no-tillage with a December manure application: NTD, no-tillage with a January manure application: CTJ. Liquid dairy manure (dry matter 2-6%) was supplied from the Emmons Blaine Dairy Facility at the University of Wisconsin Arlington Agricultural Research Station and applied by hand at a rate of 37.4 kL ha^{-1} (4000 gal ac^{-1}). All field operations were performed along the contour (i.e. planting, tillage, harvest, and manure application).

Instrumentation

Atmospheric, soil, and hydrologic parameters were measured with a combination of automated and manual instrumentation at the field site; only instruments relevant to this albedo study will be described here. An on-site weather station was equipped with an air temperature and vapor pressure sensor (model VP-3, Decagon Devices Inc., Pullman WA); a sonic anemometer (model DS-2, Decagon Devices Inc., Pullman WA); and a tipping-bucket rain gauge (model RG3, Onset Computer Corporation, Bourne, MA) modified to measure snowfall as the liquid equivalent (model CS705, Campbell Scientific, Inc., Logan, UT). The weather station was programmed to scan every minute and store hourly averages of air temperature (˚C), vapor pressure (kPa), wind speed (m s^{-1}), and wind direction (˚), and the total hourly precipitation (mm) with a datalogger (model CR1000, Campbell Scientific, Inc., Logan, UT). Each of the 18 plots was monitored for soil frost development with a frost tube (Rickard and Brown, 1972; MacKay, 1973) that was located in the 10^{th} row of corn of each plot. Three snow sticks were installed in each plot at corn rows 5, 10, and 15 for the manual measurement of snowpack depth to the nearest mm. To calculate the snow-water equivalent (SWE), defined as the height of water stored as snow in mm, the density of the snow (g cm^{-3}) was measured in each plot with a snow corer (ID = 7 cm). These manual measurements of frost and snow were collected at a minimum of once per week during the freezing season and up to daily during precipitation and thaw events. In one plot per treatment (i.e. 6 plots), an infrared radiometer (model SI-111, Apogee Instruments, Logan, UT) measured the surface temperature (soil or snow, when present). The infrared radiometer was mounted at a 1.2 m height, measured temperature every minute, and hourly averages were recorded with a datalogger (model CR1000, Campbell Scientific, Inc., Logan, UT). During the freezing season of 2015-2016, one net radiometer (model NR01, HuksefluxUSA, Center Moriches, NY) was mounted above one of the six plots per treatment at a 30 cm height and rotated to a new plot as feasible. Three net radiometers (model NR01, HuksefluxUSA, Center Moriches, NY) were used during the freezing season of 2016-2017, all of which were mounted above one of the six plots per treatment and rotated as needed. From the net radiometers, hourly averages of incoming and outgoing shortwave (SW_{IN} and SW_{OUT}, respectively) and long wave radiation (LW_{IN} and LW_{OUT}, respectively), surface temperature, and albedo were recorded with dataloggers (model CR10X, Campbell Scientific, Inc., Logan, UT).

Using a 1 x 1 m quadrat, a representative and undisturbed area within each plot was selected at random. A digital image of the quadrat was then photographed with a cellphone camera (model Samsung Galaxy 5S, Samsung Electronics Co., Ltd., Suwon, South Korea), in which all automatic settings were turned off (i.e. flash, high dynamic range (HDR), low light detection, and selective focus) and the ISO was set to 800. For plots with net radiometers, the quadrat was placed directly beneath the net radiometer and a second image was photographed for that plot. A reflectance plate (model Spectralon Targets #SRT-99-120, Labspere, Inc., North Sutton, NH) was used to verify even pixel distribution. All images were then

processed with open-source ImageJ software (Schindelin et al., 2015) using the Fiji image processing package (Schindelin et al., 2012). Each image was corrected for any distortions with Interactive Perspective, cropped to 2.25 M pixels (1500 x 1500 pixels) within the quadrat, and an RGB Histogram of the 8-bit (0-255) pixel values was plotted, with 0 representing black and 255 representing white ends of the color spectrum. The pixel mean, standard deviation, minimum, maximum, and mode were recorded.

Statistical Analysis and Modeling

The MLR was developed with 110 ground-truthed data points using a linear mixed model with R Statistical Software (R Core Team, 2014): $Y = \beta_0 + \beta_1 X_1 + \beta_2 X_2 + \cdots + \beta_i X_i$ Eq. 1

where the response variable, Y, is the measured albedo, β_0 is the statistically determined intercept, and X_i are the explanatory variables with slope β_i. 18 potential explanatory variables were identified: digital image data (pixel mean values, time, date, and year), weather (air temperature, vapor pressure or relative humidity), sky condition (sunny or overcast, incoming shortwave and longwave radiation), snow (snow depth, density, water equivalent, age), manure (presence and application timing), tillage (conventional or no-tillage), and solar position (zenith angle, declination angle, solar noon, and azimuth).

The assumptions of the MLR were then tested with the following procedures: 1) linearity and transformations were tested with a scatterplot matrix, 2) equal variance was tested with residual versus fitted plots, 3) normality was tested with quantile-quantile (QQ) plots, 3) leverage through Cook's Distance and the Bonferroni Outlier Test ($\alpha = 0.05$) were used to check for outliers, and 4) variance-inflation factors (VIF) were used to test for multicollinearity. To cross-validate the MLR, the data were partitioned with an 80/20 split. 88 of the 110 data points were randomly assigned as the Training Set, with which the explanatory variables were selected through Subset Model Selection and estimates of coefficients were calculated. The remaining 22 data points were reserved as the Test Set, which was used to evaluate the predictive error of the model by calculating the root mean squared error (RMSE). A final model was determined using the Bayesian Information Criterion (BIC), R_{adj}^2, and RMSE selection criteria.

RESULTS

Albedo Measurement and Modelling

Six explanatory variables were significant to the MLR model: the solar declination angle, manure application timing (control, December, and January), presence of manure (visually present or absent), mean pixel value of the digital image, snow depth, presence of overcast versus clear sky, and air temperature. The summary statistics of the input data are shown in Table 1, estimates of the coefficients are shown in Table 2, and the ANOVA table is shown in Table 3. The assumptions of the MLR – linearity, equal variance, and normality – were met. For all data points, Cook's Distance was less than 1, the Bonferroni outlier test was not significant ($p = 0.86796$), and multicollinearity was low (VIF < 10) (Table 1). When comparing the observed versus predicted albedo estimates, $R^2 = 0.87$ (Figure 2).

The explanatory variables in this MLR are accessible for most plot-scale, agricultural research. The solar declination angle, DEC, which is defined as the angle between the equatorial plane of the earth and the rays of the sun, controls the change in seasons and is calculated as a function of the day of the year, *J* (Campbell and Norman, 1998):

$DEC = \sin^{-1}\left[0.39785 * sin\left(278.97 + 0.9856 * J + 1.9165 * sin(356.6 + 0.9856 * J)\right)\right]$ Eq. 2

This angle is significant because it represents the location of the sun in the sky; as the sun angle decreases, albedo tends to increase. The manure inputs were developed with a simple rating system. The unmanured

control plots had a value of one, the plots with December manure application were rated two, and the plots with January manure applications were rated three. The 'presence of manure' explanatory variable was a visual rating of zero if no manure was visible in the digital image and one if manure was visually present in the image. The SKY explanatory variable was also a visually-based, binary rating system, with zero assigned to overcast sky and one assigned to clear sky. SKY was significant due to the partitioning of direct and diffuse solar radiation and subsequent albedo measurements. Overcast skies result in diffuse radiation, which increases albedo relative to clear skies (Grenfell et al., 1994; Brandt et al., 2005).

This albedo model is appropriate when snow is present, which can range from discrete patches and thin dustings of new snowfall (< 1 mm – below the measureable limit) to thick, continuous snowpack layers with or without the presence of manure and corn stalks. Bare soil is not represented by this model. At values less than 0.1, albedo becomes a nonlinear and is a well-established function of soil moisture content (Idso et al., 1975; Lobell and Asner, 2002). Snow depth was the only significant snow parameter to the MLR. Other common - but more rigorous snow measurements - such as SWE and snow age, were not significant because the values of these variables change at inconsistent rates relative to changes in albedo. For example, the albedo of snow is the highest after a new snowfall, but snow ages (i.e. darkens) at different rates according to intensity of the weather conditions, especially during melt events. Snow that undergoes a mild melt event, such as air temperature near freezing, overcast sky, and on dates near the winter solstice when solar radiation is of minimal intensity, ages more slowly than snow that undergoes an intense melt event, such as air temperature several degrees above freezing, clear sky, and on dates closer to the spring equinox when solar radiation is of greater intensity. Moreover, evidence suggests that snow properties, such as grain size, which is a function of snow age, does not have as strong of an effect on albedo as broader controls, such as the sun angle and snow depth (Brandt et al., 2005).

This MLR provides an inexpensive, replicable method to quantify albedo in plot-scale research on a field with corn for silage. Most snow albedo models have been developed in the arctic, Antarctica, and alpine regions with glacial landscapes, which experience deeper, continuous snowpack compared to temperate, agricultural fields with thin snowpack that undergoes frequent melt events and various field operations.

Example Use: Radiative Energy and Treatment Effects

The MLR was used to calculate the albedo of all of the plots in this study and quantify the effect of the manure on resultant shortwave, longwave, and net radiation. The following calculations were made:

$$R_{NET} = (SW_{NET}) + (LW_{NET}) \quad \text{Eq. 3}$$

where R_{NET} is net radiation, SW_{NET} is net shortwave radiation, and LW_{NET} is net longwave radiation, all units are in W m^{-2}, and

$$SW_{NET} = SW_{IN} - SW_{OUT} \quad \text{Eq. 4a}$$

$$SW_{OUT} = \alpha SW_{IN} \quad \text{Eq. 4b}$$

$$LW_{NET} = LW_{IN} - LW_{OUT} \quad \text{Eq. 4c}$$

$$LW_{OUT} = \varepsilon \sigma \boldsymbol{T}^4 \quad \text{Eq. 4d}$$

where SW_{IN} is incoming shortwave radiation that is measured directly from the net radiometers and SW_{OUT} is outgoing shortwave radiation that is calculated from albedo, α, from the MLR. LW_{NET} is net longwave radiation, which is calculated from direct measurement of incoming longwave radiation (LW_{IN}) from the net radiometers; an assumed emissivity, ε = 0.97 (Campbell and Norman, 1998); the Stefan-Boltzmann

constant, $\sigma = 5.67 \times 10^{-8}$ W m^{-2} K^{-4}; and **T**, the surface temperature of each treatment in Kelvin measured by the infrared radiometers. Therefore, data related to shortwave radiation were calculated for each plot and the plot data were used to calculate the averages and standard error across the manure and tillage treatments. The data related to longwave radiation were restricted to one value per treatment because there was only one infrared radiometer (surface temperature measurement) per treatment.

The albedo of the plots ranged from 0.08, for bare, saturated, thawing soil without snowpack to 0.95 for freshly fallen snow. The application of liquid dairy manure (2-6 % dry matter) at a rate of 37.4 kL ha^{-1} resulted in a patchy, discontinuous layer of manure that infiltrated the underlying snowpack. The first manure application on top of snowpack took place January 26, 2016, the morning after a snowfall with a 7.4 mm water equivalent, from which over 10 cm of new snowpack accumulated across the plots. A single net radiometer recorded the change in albedo from 0.95 of the freshly fallen snow to 0.33 in a plot under no-tillage with a January manure application. The subsequent albedo in that plot had a daily average of 0.37 (SD =0.02) on January 27, 0.39 (SD = 0.05) on January 28, and 0.36 (SD = 0.04) on January 29, whereas the albedo of unmanured snowpack remained above 0.89. Beginning on January 30, a snowmelt event occurred and the albedo decreased to 0.12 by February 1, 2016, in the manured plot and the unmanured snowpack dropped to 0.46. On February 4, 2016, a new snowfall event occurred and on February 7, 2016, a new snowmelt event began. An efficient method to capture these abrupt changes in albedo was clearly needed, thus led to the creation of the digital imagery method on February 8, 2016. Despite starting the digital albedo measurements after two melt events post-manure application, the manure exhibited a legacy effect on albedo through February 15, 2016. By February 18, 2016, the next date of digital imagery, a large-scale snowmelt event occurred, in which all of the snowpack melted. After the mid-February 2016 event, the January-manured plots were not significantly different from the controls and December-manured plots. By testing the efficacy of the digital imagery in late winter 2015-2016, a more rigorous campaign was completed for the winter of 2016-17 and will be the focus of the radiation analysis.

On December 9, 2016, the albedo of conventional tillage plots with the December manure application timing treatment, CTD, decreased from 0.71 (SE ± 0.00) to 0.46 (SE ± 0.04) and no-tillage plots with the December manure application timing treatment, NTD, decreased from 0.69 (SE ±0.01) to 0.39 (SE ±0.04) (Figure 4). On January 27, 2017, the albedo of CT with the January manure application timing treatment, CTJ, decreased from 0.73 (SE ± 0.02) to 0.45 (SE ± 0.04) and NT plots with the January manure application timing treatment, NTJ, decreased from 0.74 (SE ±0.01) to 0.48 (SE ±0.01) (Figure 4). After new snowfall, all of the plots had similar albedos, but as the snow aged, the albedo of the plots with the January manure application timing remained lower than that of the plots with other manure application timings, with albedo from January applications remaining 0.51 to 0.41 lower in the CT and NT plots, respectively, than plots with December manure applications and controls in February three weeks later (Figure 4).

The average daily outgoing shortwave radiation ranged from 3 to 202 W m^{-2} throughout the winter of 2016-17. Differences in the average daily outgoing shortwave radiation became pronounced after the January, but not the December, manure application across tillage treatments. On January 27, 2017, the outgoing shortwave radiation, hence net shortwave radiation, was reduced by an average of 36.4 (SE ±3.6) W m^{-2} in the plots under CTJ compared to CTC and by 35.0 (SE ±1.3) W m^{-2} in the plots under NTJ compared to NTC. During subsequent snowmelt events, the difference in outgoing and net shortwave radiation increased between the plots with January manure applications and unmanured controls. A maximum difference of 75.8 (SE ±6.1) W m^{-2} was reached on Feb 12, 2017 between CTJ and CTC, and maximum difference of 96.2 (SE ±1.3) W m^{-2} was reached a day later, on Feb 13, 2017, between NTJ and NTC. Of the unmanured control plots and plots with a December manure application timing, differences were not significant within tillage, but average daily outgoing shortwave radiation was 20-50 W m^{-2} greater in no-

tillage compared to conventional tillage by the mid-February melt event. Tillage with a fall chisel plow creates a network of ridges and furrows and the presence of the ridges tends to lower albedo (Figure 4), allowing for greater absorption of shortwave radiation (i.e. less outgoing). Snow tends to be thinner on the ridges because of drift during accumulation and this thinner layer of snow then tends to regress faster during melts, exposing the underlying dark, bare soil. Under no-tillage, snowpack is tends to stabilize as a thicker, continuous layer unless manure is added in late January.

The application of liquid dairy manure lowered albedo, which increased energy absorption from shortwave radiation, but did not change longwave radiation dynamics. Therefore differences in net radiation are solely a result of changes to shortwave radiation absorption and were most significant after the January manure applications (Figure 5). The average daily net radiation was 30 W m^{-2} greater in plots with January manure applications versus unmanured controls and December applications during the February 8, 2017, melt event and 60 W m^{-2} greater during the February 12, 2017, melt event, or double that of the unmanured controls and December applications. Cumulative across the course of the winter season in the plots with conventional tillage, the average daily net radiation was 31 W m^{-2} greater in the plots with a December manure application compared to the unmanured control plots and 536 W m^{-2} greater in the plots with a January manure application compared to the unmanured control plots (Figure 5). For plots with no-tillage, the average daily net radiation was 90 W m^{-2} greater in the plots with a December manure application compared to the unmanured controls and 701 W m^{-2} in the plots with a January manure application compared to the unmanured controls. Because this increase in absorbed radiative energy did not contribute to heating a discrete, insulative manure layer (as with solid, bedded manures), the energy was transmitted to the snowpack, increasing the energy available for melt. As a result, snowmelt accelerated, which may increase the risk of surface runoff and nutrient transport on frozen soils that have a reduced infiltration potential. During the 2015-16 season, snowmelt was complete one to two days earlier in January-manured plots and during the 2016-17 season, snowmelt ended up to three days sooner, with 8 mm of SWE melting per day, or snowpack depths of 2-5 cm per day.

Conclusion

The winter-application of manure to the landscape is a long standing practice, but relatively little research has investigated the physical processes that control snowmelt, hence drive runoff, in relation to manure applications. This research demonstrated a new method using a MLR with digital imagery and readily obtained site characteristics to estimate albedo in plot-scale, agricultural research with dynamic snow behavior and field operations. As an application of the MLR method, a radiative energy balance was completed while testing the behavior of liquid dairy manure (2-6 % dry matter) that was applied early in the freezing season versus later and the resultant radiative balance on agricultural soils with snowpack. Early applications of manure (i.e. December) did not alter the radiative energy at the surface longer than the day of the application, whereas late applications of manure in January produced an immediate and legacy effect on albedo. As late winter applications of manure lowered albedo, the outgoing shortwave radiation decreased, which resulted in greater net radiation absorbed by the snowpack and subsequent energy available for snowmelt. Because liquid manure both disperses within snowpack and has a high thermal conductivity, a mulching effect is not observed, as with solid, bedded manure application on top of snowpack. Therefore, applications of liquid manure may increase runoff and pose a challenge for nutrient transport from the manure during thaw events.

REFERENCES

Brandt, R.E., S.G. Warren, A.P. Worby, and T.C. Grenfell. 2005. Surface albedo of the Antarctic Sea Ice Zone. J Climate 18: 3606-3622.

Campbell, C.S. and J.M. Norman. 1998. An Introduction to Environmental Biophysics. Springer Science + Business Media, LLC. New York, New York, 286 pp.

Carpenter, S.R., N.F. Caraco, D.L. Correll, R.W. Howarth, A.N. Sharpely, and V.H. Smith. 1998. Nonpoint pollution of surface waters with phosphorus and nitrogen. Ecol. Appl. 8(3): 559-568.

Corripio, J.G. 2004. Snow surface albedo estimation using terrestrial photography. Int J Remote Sensing 25(24): 5705-5729. DOI: 10.1080/01431160410001709002

Good, L.W., P. Vadas, J.C. Panuska, C.A. Bonilla, W.E. Jokela. 2012. Testing the Wisconsin Phosphorus Index with Year-Round, Field-Scale Runoff Monitoring. J. Environ. Qual. 41: 1730-1740.

Grenfell, T.C., S.G. Warren, and P.C. Mullen. 1994. Reflection of solar radiation by the Antarctic snow surface at ultraviolet, visible, and near-infrared wavelengths. J Geo Res 99(D9): 669-684.

Idso, S.B., R.D. Jackson, R.J. Reginato, B.A. Kimball, and F.S. Nakayama. 1975. The dependence of bare soil albedo on soil water content. J App Met 14: 109-113.

Kongoli and Bland, 2002 Kongoli, C.E., and W.L. Bland. 2002. Influence of manure application on surface energy and snow cover: Field experiments. J. Environ. Qual. 31:1166-1173.

Lobell D.B. and G.P. Asner. 2002. Moisture effects on soil reflectance. Soil Sci Soc Am J 66(3): 722-727. doi:10.2136/sssaj2002.7220

MacKay, J.R. 1973. A frost tube for the determination of freezing in the active layer above permafrost. Canadian Geotechnical Journal 10:392–396.

Parris, K. 2011. Impact of Agriculture on Water Pollution in OECD Countries: Recent Trends and Future Prospects. Int. J. Water Resour. D. 27: 33-52. doi:Pii 933159867.

Rickard, W. and J. Brown. 1972. The performance of a frost-tube for the determination of soil freezing and thawing depths. Soil Science. 113(2):149–154.

Srinivasan, M.S., R.B. Bryant, M.P. Callahan, and J.L. Weld. 2006. Manure management and nutrient loss under winter conditions: A literature review. J. Soil Water Conserv. 61:200-209.

Stuntebeck, T.D., M.J. Komiskey, M. C. Peppler, D.W. Owens, and D.R. Frame. 2011. Precipitation-runoff relations and water quality characteristics at edge-of-field stations, Discovery Farms and Pioneer Farm, Wisconsin, 2003-2008. U.S.G.S. Scientific Investigations Report 2011-5008.

USEPA. 2015. US EPA Watershed Assessment, Tracking, and Environmental Results. Retrieved from: http://ofmpub.epa.gov/waters10/attains_nation_cy.control

TABLES AND FIGURES

Table 1. Summary statistics of the explanatory variables in the multiple linear regression, including the mean, standard deviation (SD), minimum (Min), maximum (Max), Median, and corresponding variance-inflation factors (VIF). Statistics are only reported for the explanatory variables that were significant to the model.

Explanatory Variable	Description	Mean	SD	Min	Max	Median	VIF
DAY†	Day of Year	Jan 25	29	Dec 5	Mar 25	Jan 27	1.6
DEC	Solar declination Angle [˚] ϕ	-16.9	6.6	-23.4	1.8	-18.7	1.7
ManureApp	Manure Application Timing: 1 = Unmanured control 2 = December 3 = January	2.4	0.6	1	3	2	1.1
ManurePresent	Manure Presence: 0 = Not visible in image 1 = Visible in image	0.4	0.5	0	1	0	1.4
PixelMean	Mean RGB Value of Pixels	136.3	29.3	74.8	206	135.9	2.5
SnowDepth	Snow Depth [mm]	95.7	72.4	0*	231	79	2.6
Sky	Sky Conditions: 0 = overcast 1 = clear, sunny	0.4	0.5	0	1	0	1.3
T_{AIR}	Air Temperature [˚C]	-1.9	4.3	-16.2	8.2	-1.4	1.1

† Expressed as the day of year in the MLR

ϕ $DEC = \sin^{-1}\left[0.39785 * sin\left(278.97 + 0.9856 * J + 1.9165 * sin(356.6 + 0.9856 * J)\right)\right]$ (Campbell and Norman, 1998)

* Zero represents snow that was present as a light dusting, but snow depth was below detection with instrumentation

Table 2. Summary statistics of the multiple linear regression model, including the estimate of each coefficient with standard error (SE), T-Value, and P-Value by explanatory variable. The R^2, R_{adj}^2, Bayesian Information Criterion (BIC) were calculated from the Training Set (88 data points, 80% of the data), and Root Mean Squared Error (RMSE) was calculated from the Test Set (22 data points, 20% of the data) for the model as a whole.

Explanatory Variable	Estimate	SE	T-Value	Pr (> |t|)
Intercept	0.01824	0.0809570	0.225	0.8223
Day	0.0003779	0.0000825	4.581	< 0.0001
Declination	-0.004518	0.0017949	2.517	0.0139
ManureApp	-0.04301	0.0163344	2.633	0.0102
ManurePresent	-0.1139	0.0250986	-4.538	< 0.0001
PixelMean	0.002997	0.0005001	5.993	< 0.0001
SnowDepth	0.001135	0.0002020	5.615	< 0.0001
Sky	-0.07453	0.0212516	-3.507	0.0008
T_{AIR}	-0.008951	0.0023514	-3.807	0.0003
			R^2 =	**0.8832**
			R_{adj}^2 =	**0.8714**
			BIC =	**-140**
			RMSE =	**0.10**

Residual standard error: 0.0867 on 79 degrees of freedom,
F-statistic: 74.7 on 8 and 79 DF, p-value: <0.0001

Table 3. The Analysis of Variance for the multiple linear regression model, including the degrees of freedon (DF), Sum of Squares (SS), Mean Squares (MS), F Value, and P-value by each explanatory variable with residuals.

Variable	DF	SS	MS	F Value	Pr(>F)
Intercept	1				
Day	1	1.05016	1.05016	139.6953	< 0.0001
Declination	1	0.3038	0.30378	40.4099	< 0.0001
ManureApp	1	0.04217	0.04217	5.6099	0.0203
ManurePresent	1	0.9724	0.97236	129.3451	< 0.0001
PixelMean	1	1.546	1.54593	205.6429	< 0.0001
SnowDepth	1	0.3358	0.33582	44.6719	< 0.0001
Sky	1	0.1336	0.13355	17.7656	< 0.0001
T_{AIR}	1	0.1089	0.10894	14.4917	0.0003
Residuals	**79**	**0.5939**	**0.00752**		

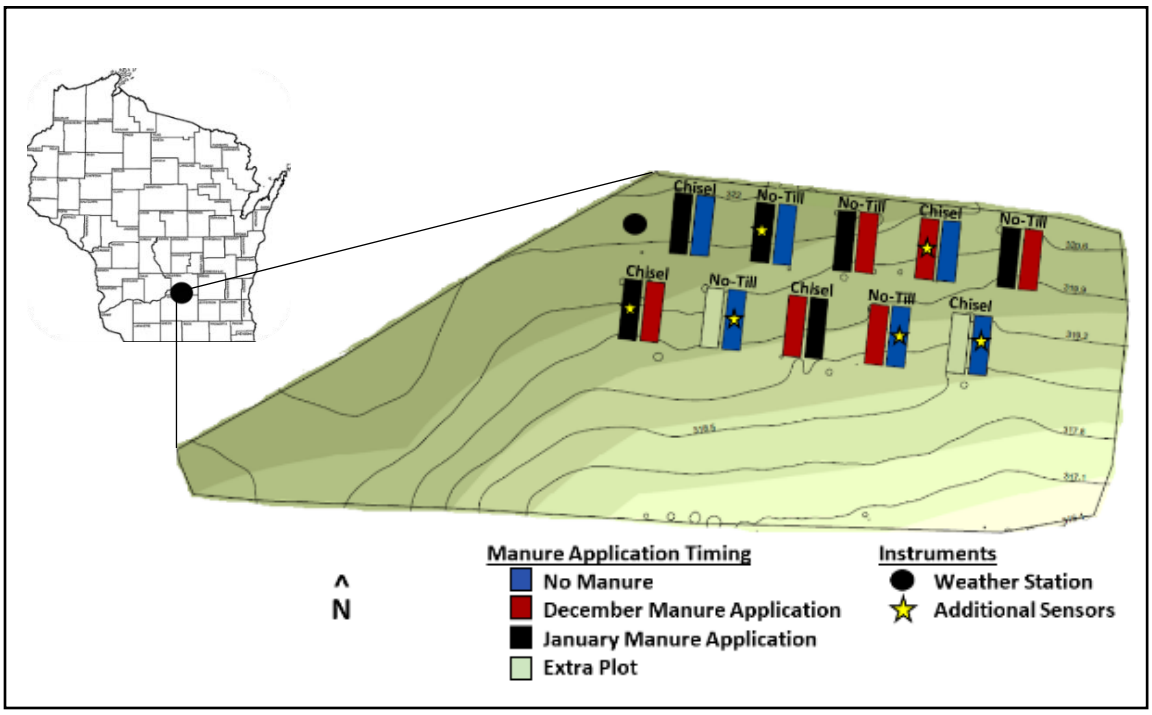

Figure 1. This study was established at the UW Agricultural Research Station in Arlington, WI, on a south-facing, 6% slope in continuous corn for silage. The 18 plots follow a complete factorial design (2 tillage x 3 manure timing treatments) in triplicate and are arranged in pairs according to tillage: Chisel = conventional tillage with a fall chisel plow and a spring finsher, and No-Till = no-tillage. Within the pairs, the manure application timings are randomized. The field contains one weather station and one plot per treatment (designated with a star) is equipped with additional instrumentation.

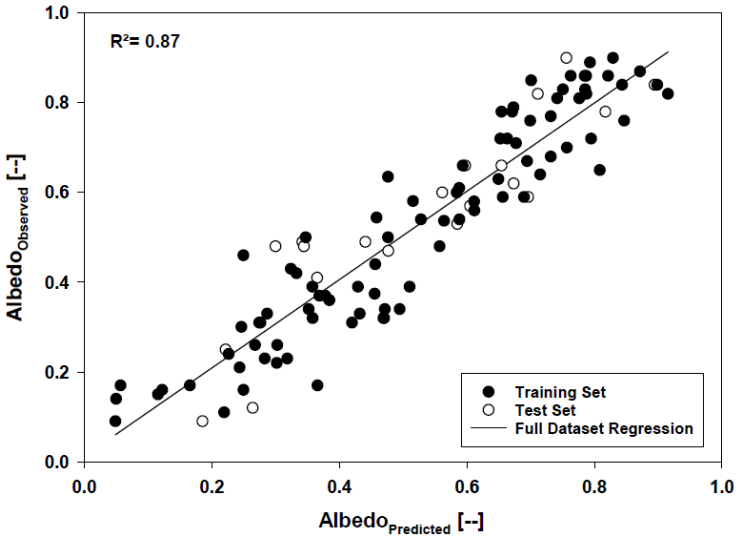

Figure 2. The observed versus predicted albedo from the MLR. 80 % of the data (88 data points) were used in the Training Set to fit the model (black circles) and 20 % (22 data points) were used as the Test Set to validate the model (white circles). R^2 = 0.87 for the full dataset across 40 days in 2016-2017.

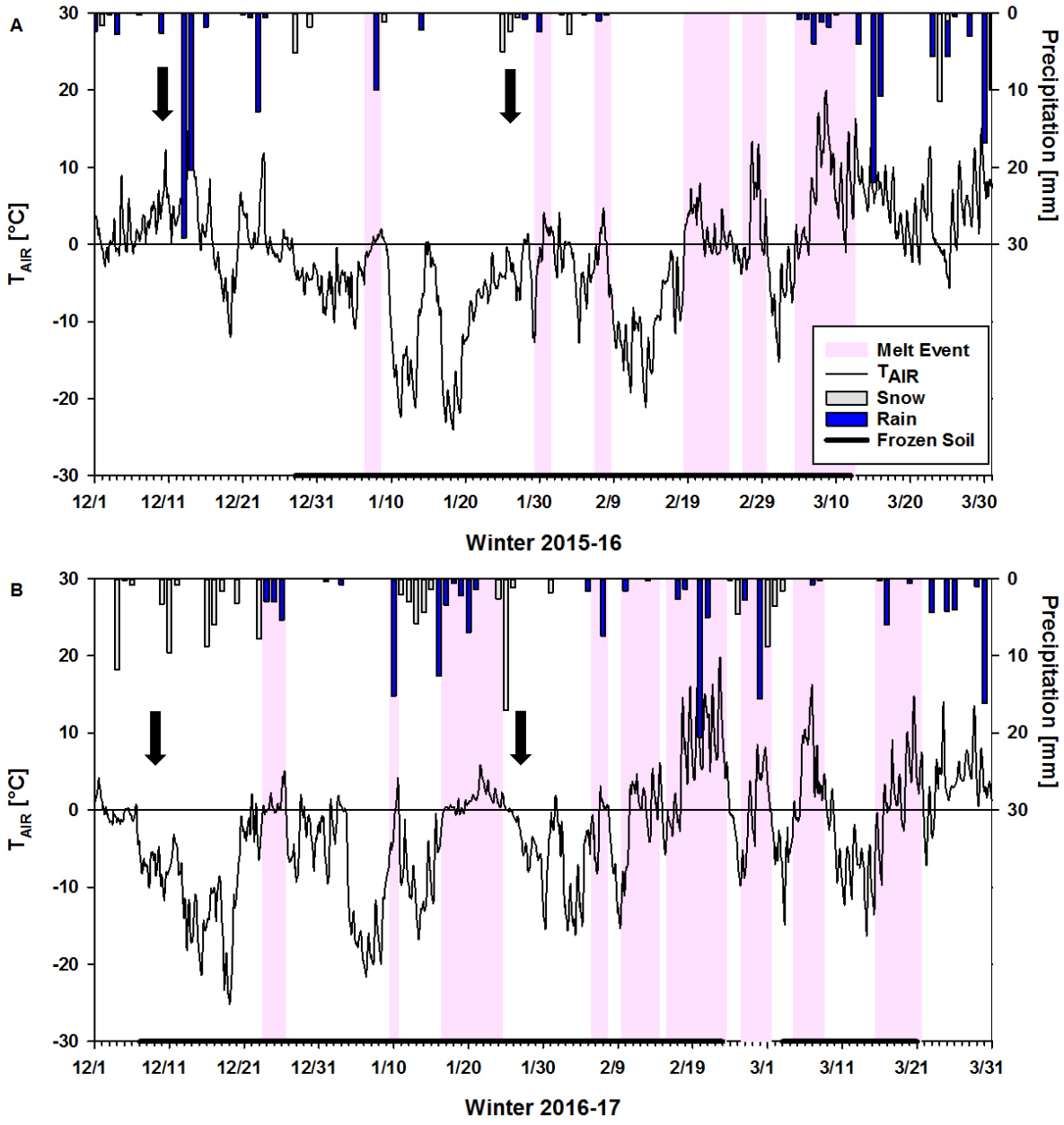

Figure 3. The weather and melt conditions during Winters 2015-16 and 2016-17, including air temperature, T_{AIR}, in ˚C; precipitation as rainfall (blue bar plot) or the liquid equivalents of snowfall (gray bar plot) in mm, the presence of frozen soil (thick black line plot) and melt events during the freezing seasons (pink shading). The black arrows indicate the dates of dairy manure applications, which include Dec 10, 2015, January 26, 2016, Dec 9, 2016, and January 27, 2017.

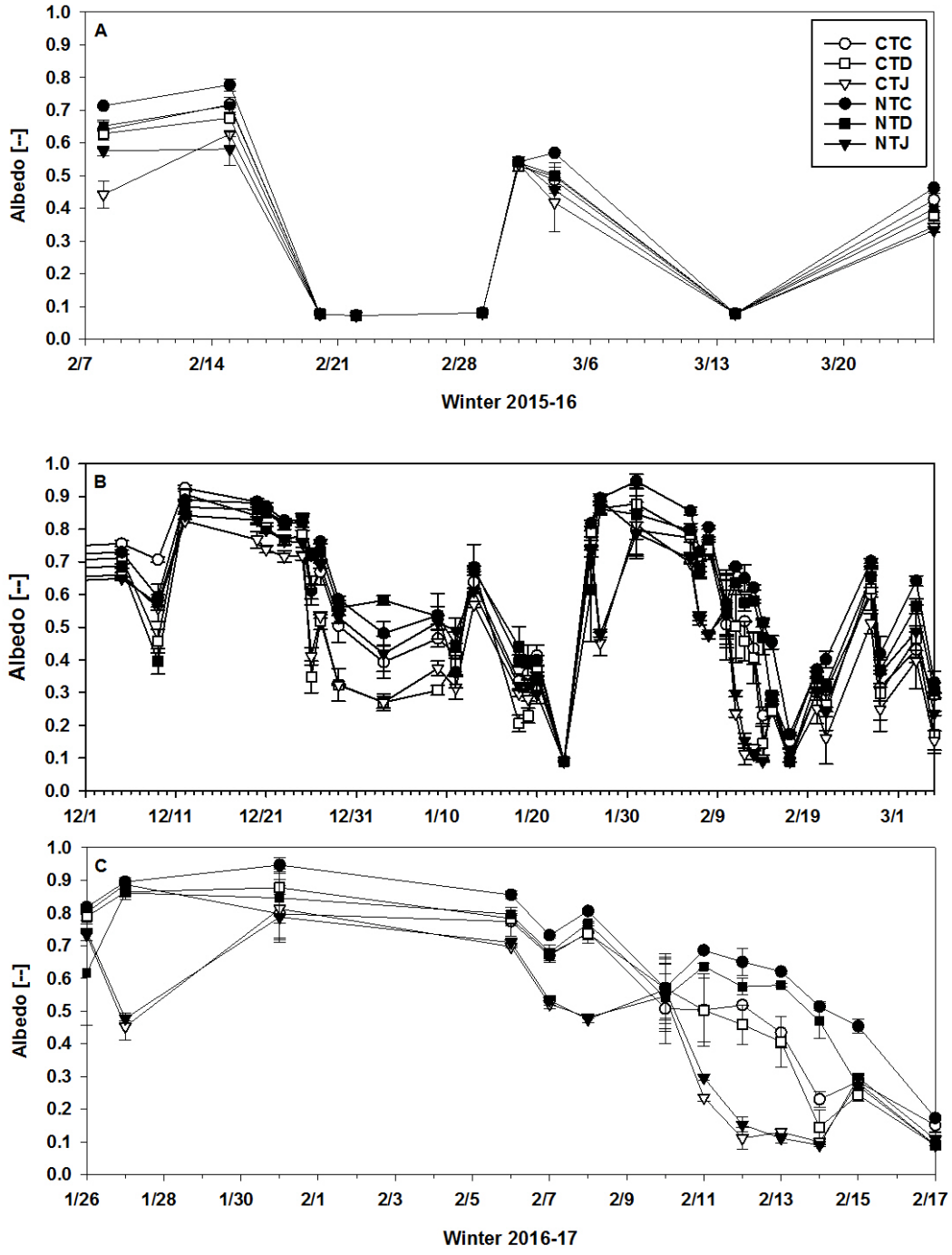

Figure 4. The average albedo (± SE) by tillage and manure timing treatment: conventional tillage with no manure (control), CTC, denoted with white circles; conventional tillage with a December application, CTD, denoted with white squares; conventional tillage with a January application, CTJ, denoted with white triangles; no-tillage with no manure (control), NTC, denoted with black circles; no-tillage with a December application, NTD, denoted with black squares; and no-tillage with a January application, NTJ, denoted with black triangles. A) The albedo measurements during late winter of 2015-16; B) albedo across winter 2016-17; and C) albedo after the January 2017 manure application until February 17, 2017, when the snow in all of the treatments had melted.

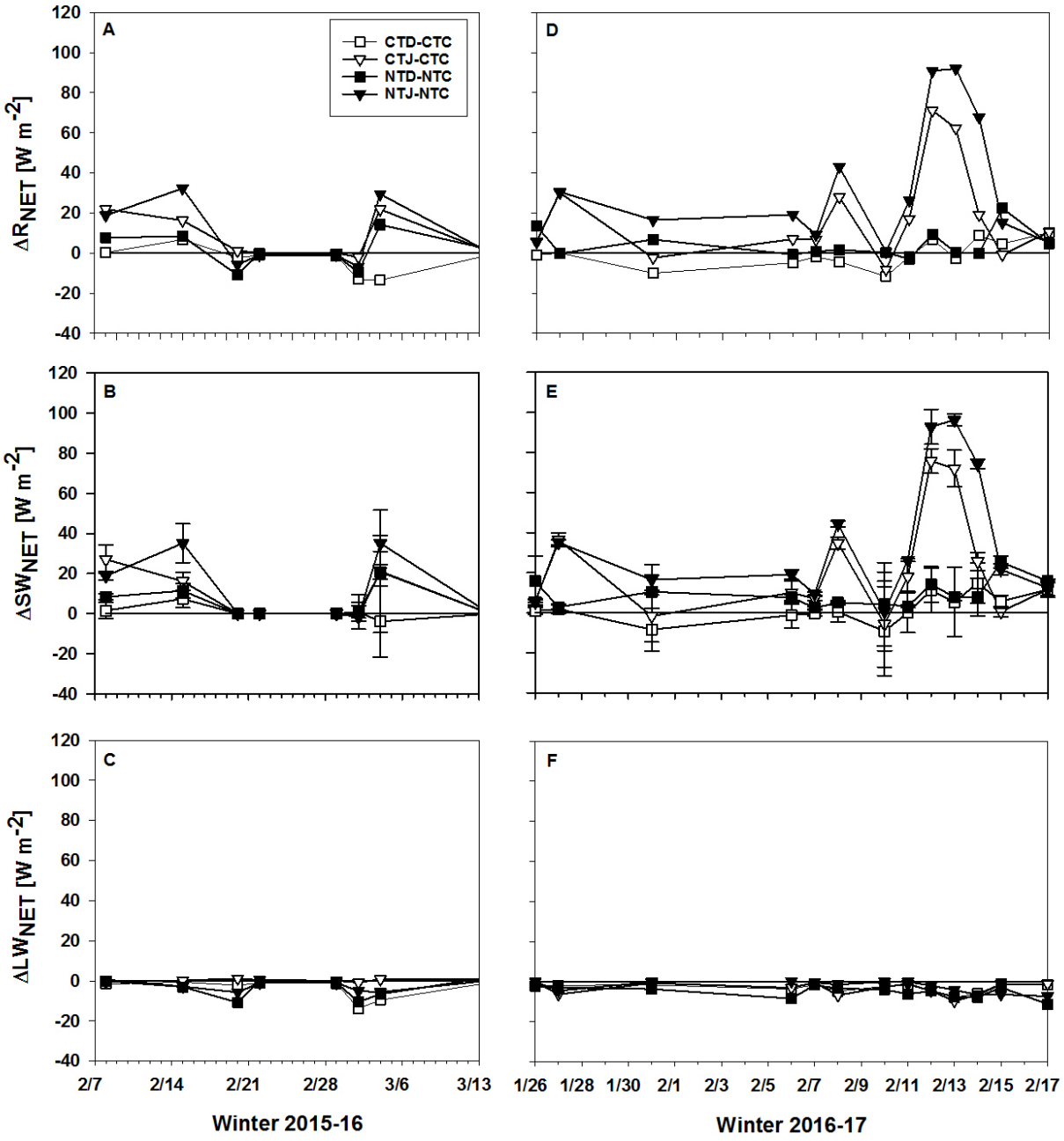

Figure 5. The difference in radiation (W m^{-2}) between the manure treatment and its unmanured control by tillage treatment with winter 2015-16 in the left panels and winter 2016-17 in the right panels. The difference between the December manure applications and the unmanured controls in the plots with conventional tillage (CTD-CTC) is denoted with a white square, the difference between the January applications and the unmanured controls in the plots with conventional tillage (CTJ-CTC) is denoted with a white triangle, the difference between the December applications and the unmanured controls in the no-tillage plots (NTD-NTC) is denoted with a black square, and the difference between the January applications and the unmanured controls in the no-tillage plots (NTJ-NTC) is denoted with a black triangle. A) The difference in net radiation, ΔR_{NET}, B) the difference in average net shortwave radiation (±SE), SW_{NET}, and C) the difference in net longwave radiation, LW_{NET} after the January manure application in 2017.